Underwater Information Sensing Method Based on Improved Dual-Coupled Duffing Oscillator Under Lévy Noise Description

Hanwen Zhang[1(✉)], Zhen Qin[2,3], and Dajiang Chen[2,3]

[1] School of Automation Engineering, University of Electronic Science and Technology of China, Chengdu, Sichuan, China
201952060908@std.uestc.edu.cn
[2] Network and Data Security Key Laboratory of Sichuan Province, University of Electronic Science and Technology of China, Chengdu, Sichuan, China
[3] School of Information and Software Engineering, University of Electronic Science and Technology of China, Chengdu, Sichuan, China

Abstract. Sensing underwater information has become particularly important to obtain information about the marine environment and target characteristics. At present, most interference models for underwater information sensing tasks under substantial interference choose Gaussian noise models. However, it often contains a strong impact and does not conform to the Gaussian distribution. Moreover, in the current research on the sensing of underwater unknown frequency signals, there are problems that the sensing method cannot sufficiently estimate the parameters of the unknown frequency signal, and the signal-to-noise ratio threshold is too high. An underwater environment sensing method is proposed by using the Lévy noise model to describe the underwater natural environment interference and estimate its parameters, which can better describe the impact characteristics of the underwater environment. Then, the intermittent chaos theory and variable step method are leveraged to improve the existing dual-coupled Duffing oscillator method. The simulation results show that the proposed method can sense weak signals in the background of strong Lévy noise and estimate its frequency, with an estimation error as low as 0.1%. Compared with the original one, the minimum signal-to-noise ratio threshold is reduced by 3.098 dB, and the computational overhead is significantly reduced.

Keywords: Underwater information sensing · Lévy noise · Dual-coupled Duffing oscillator

1 Introduction

With the improvement of modern technology, e.g., Internet of Things (IoT) [1–3] and Artificial Intelligence (AI) [4, 5], people have begun to develop and utilize marine resources [6, 7]. Therefore, domestic and foreign personnel have conducted extensive research on underwater target technology to sense the underwater environment and exploit underwater resources [8, 9]. Nowadays, most of the research chooses the Gaussian noise model for discussion. This is because non-Gaussian noise does not have

H. Gao and X. Wang (Eds.): CollaborateCom 2021, LNICST 406, pp. 156–170, 2021.
https://doi.org/10.1007/978-3-030-92635-9_10

Markov characteristics and is extremely difficult to process in weak signal sensing research [10]. Noise interference in the underwater environment often contains intense pulses, which do not conform to the Gaussian distribution [11–13]. The Lévy distribution is a generalized form of the Gaussian distribution. It has broader applicability than the Gaussian distribution, and it is the only distribution that satisfies the generalized central limit theorem among all distributions. The Lévy noise is a typical non-Gaussian noise with long tails, discontinuous jumps, and infinite separability. It can maintain the natural noise process's generation mechanism and propagation conditions and align with the actual situation. The Levy noise model established by the Lévy distribution can describe many symmetrical or asymmetrical noises with different impulse degrees by controlling the selection of different parameters, which can better describe the impact characteristics of underwater environmental noise interference, is of great significance to the research of underwater information sensing. Plus, in the current research on the sensing of underwater unknown frequency signals, there are problems that the sensing method cannot sufficiently estimate the parameters of the unknown frequency signal, and the signal-to-noise ratio threshold is too high [14–18].

This paper proposes a more in line with the weak signal sensing of underwater position in the complex marine environment to solve problems mentioned above. The main contributions of this article are as follows:

1. Propose the Lévy noise model to describe the interference of the underwater natural environment and provide a method to analyze, estimate and select parameters that are closer to the actual underwater natural environment interference.
2. Aiming at sensing weak underwater signals with unknown frequencies, an improved signal sensing method of dual-coupled Duffing oscillators is proposed, which is more effective and intuitive.
3. Designed and established a sensing system for weak signals of unknown frequencies underwater based on the improved dual-coupled Duffing oscillator under the interference of the Lévy noise model and verified its feasibility and supriority.

2 Related Work

2.1 Lévy Noise Model

The Lévy process was proposed by the French mathematician Paul Lévy to study of the generalized central limit theorem. It is a random process with independent and fixed increments, indicating that the movement of a point and its continuous displacement are random. The difference between two disjoint time intervals displacement is independent. The displacement and displacement in different time intervals of the same length have the same probability distribution. It can be regarded as a continuous-time simulation of random walk. Lévy noise, also called alpha noise, obeys the theory of stable alpha distribution. The only distribution satisfies the generalized central limit theorem, and a square law attenuates its tailing. The expression of the characteristic function of Lévy noise [19] is as follows:

$$\log\varphi(t) = \begin{cases} -\sigma^{\alpha}|t|\left\{1 - i\beta\mathrm{sign}(t)\tan\left(\frac{\pi\alpha}{2}\right)\right\} + i\mu t, \alpha \neq 1 \\ -\sigma^{\alpha}|t|\left\{1 + i\beta\mathrm{sign}(t)\frac{\pi}{2}\log(|t|)\right\} + i\mu t, \alpha = 1 \end{cases} \tag{1}$$

$$\begin{cases} X = S_{\alpha,\beta}\frac{\sin\left(\alpha\left(V + B_{\alpha,\beta}\right)\right)}{(\cos V)^{\frac{1}{\alpha}}}\left(\frac{\cos\left(V - \alpha\left(V + B_{\alpha,\beta}\right)\right)}{W}\right)^{\frac{1-\alpha}{\alpha}}, \alpha \neq 1 \\ X = \frac{2}{\pi}\left[\left(\frac{\pi}{2} + \beta V\right)\tan V - \beta\log\left(\frac{W\cos V}{\frac{\pi}{2} + \beta V}\right)\right], \alpha = 1 \end{cases} \tag{2}$$

In (1), $\alpha \in [0, 2]$ is the characteristic index, which determines the decay rate of the distribution tail. When $\alpha = 1$, it is Cauchy distribution. When $\alpha = 2$, It is the Gaussian distribution, and the mean value is μ, the variance is 2 σ^2. when $\alpha \neq 2$, the mean value is μ, but the variance does not exist. $\beta \in [-1, 1]$ is the skew parameter. When $\beta = 0$, the graph is symmetrical, and when β is a positive number, The graph tilts to the right, on the contrary, the graph tilts to the left, $\sigma > 0$ is the scale parameter, which determines the degree of dispersion of the distribution concerning μ, and $\mu \in R$ is the position parameter. The left and right translation can be achieved by adjusting the value of μ. Rfal-Weron proved the expression of Lévy distribution random variable. In (2), V obeys the uniform distribution in the interval $(-2\pi, 2\pi)$, W follows the exponential distribution with the mean value 1, $S_{\alpha,\beta}$ and $B_{\alpha,\beta}$ The definition expression is as follows:

$$S_{\alpha,\beta} = \left[1 + \beta^2\tan^2\frac{\pi\alpha}{2}\right]^{1/2\alpha} \tag{3}$$

$$B_{\alpha,\beta} = \frac{\arctan\left(\beta\tan\frac{\pi\alpha}{2}\right)}{\alpha} \tag{4}$$

Under the conditions of $\beta = 0, \sigma = 1$ and $\mu = 0$, the Lévy distributions corresponding to different α feature indices are shown in Fig. 1:

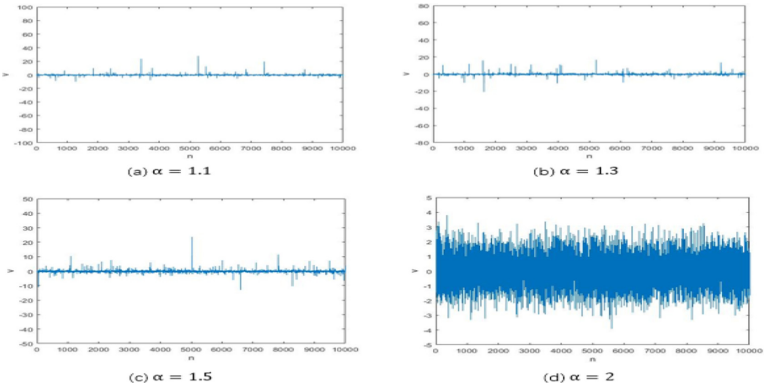

Fig. 1. Time-domain distribution map of live noise corresponding to different feature index α

It can be seen from Fig. 1 that the smaller the value α, the stronger the impact of noise interference. When $\alpha = 2$, the noise interference has almost no impact. At this time, the Lévy noise degenerates into white noise.

2.2 Chaotic Oscillator Signal Sensing System

Single Duffing Vibrator. The nonlinear dynamic system described by Duffing equation exhibits rich nonlinear dynamic characteristics, including complex oscillation dynamics, bifurcation, and chaos. The specific form of a single Duffing oscillator equation is:

$$\ddot{x}(t) + k\dot{x}(t) - x(t) + x^3(t) = F\cos(\omega t) \tag{5}$$

Where $x(t)$ is the chaotic system variable; k is the damping ratio; t is the time variable; $F\cos(\omega t)$ is the periodic driving force, where F is the amplitude of the periodic driving force, and ω is the angular frequency of the periodic driving force; $-x(t) + x^3(t)$ is the nonlinear restoring force. When k is fixed, the system's state changes regularly with the amplitude of the driving force $F\cos(\omega t)$. Measured by the simulation experiment, when F increases to 0.82673, the system enters the critical state of large-scale periodic motion. At this time, the magnitude of the driving force 0.82673 is the critical threshold for the transition from chaos to a periodic state. The signal sensing method using a single Duffing vibrator can effectively sense the signal, but the immunity to noise interference is low. If the interference is too strong, the phase trajectory will remain in a chaotic state, resulting in an illusion that the signal is not sensed, and misjudgment occurs.

Double Coupling Duffing Vibrator. The double coupling Duffing vibrator is an improved Duffing vibrator, and its specific form is:

$$\begin{cases} \ddot{x}(t) + k\dot{x}(t) - x(t) + x^3(t) + d(y(t) - x(t)) = Fcos(\omega t) \\ \ddot{y}(t) + k\dot{y}(t) - y(t) + y^3(t) + d(x(t) - y(t)) = Fcos(\omega t) + Y(t) \end{cases} \tag{6}$$

Where x is the variable of Duffing oscillator one; y is the variable of Duffing oscillator two; d is the coupling coefficient. When $d = 0$, the coupling effect of the two oscillators disappears. At this time, the dynamic behavior of the double coupled Duffing oscillator is the same as that of the single Duffing oscillator. The dynamic behavior is completely consistent; when $d \neq 0$, the variables x and y will quickly become synchronized under the influence of coupling; $Y(t)$ is the external input signal of the system, including the signal to be sensed A$s(t)$ and noise signal η(t), A is the amplitude of the signal to be sensed, and the frequency of the signal to be sensed and the driving force frequency are independent of each other. The dynamic characteristics of the dual-coupled Duffing vibrator are similar to that of the single Duffing vibrator. It also changes regularly with the driving force $F\cos(\omega t)$ amplitude when the damping ratio is fixed. However, this signal sensing method does not solve the parameter estimation of unknown frequency signals, and there is still a high signal-to-noise ratio threshold.

3 Approach

3.1 Lévy Noise Model Describes Underwater Natural Environment Interference

The Fokker-Plank equation corresponding to Eq. (1) is:

$$\frac{\partial_p(s,t)}{\partial_t} = \left[\frac{\partial}{\partial_x}A(x) + \frac{\partial^2}{\partial_x}B(x)\right]\rho(s,t) \tag{7}$$

where $A(x) = ax - bx^3 + S(x)$, $B(x) = D$. Since Eq. (7) is a transcendental equation, it cannot be solved directly, but the approximate number of Eq. (1) can be calculated using the finite difference method. Set the system parameters $a = 0.6, b = 0.3, A = 0.3, f = 0.005$, noise parameters $\alpha = 1.5, \beta = 0, \sigma = 1, \mu = 0$, the probability distribution curve of particle density is shown in Fig. 2.

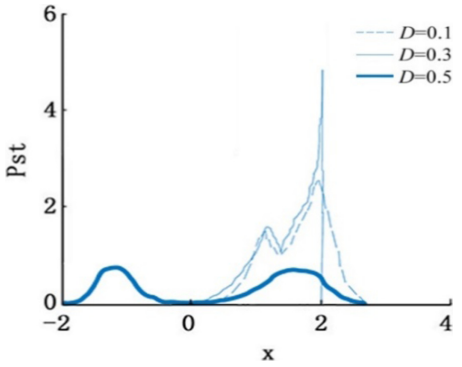

Fig. 2. The particle probability distribution of the system output under the excitation of different noise intensity D

When the Lévy noise intensity is 0, the probability distribution of particle density is only affected by the signal. When the noise intensity D increases from 0.1 to 0.3, the particle density probability shows that the particles are mainly concentrated on the side of the 0 points. When the noise intensity D reaches 0.5, the particles are unevenly distributed on both sides of 0. From the microscopic particle motion law perspective, when the noise intensity D is 0.3, the external noise excitation intensity is not enough. The energy obtained by the particle is not enough to make it cross the potential barrier and can only move left and right in a potential well, so the probability of the particle. The distribution is concentrated on the 0 sides. The resultant force of the signal pull and noise interference that the particle receives at 0 determines whether its distribution is in the left or right potential well. When the noise intensity is 0.5, the particles will be excited by solid noise. They will get enough energy to cross the potential barrier from one potential well into another potential well. At this time, the transfer of particles between potential wells will be affected by noise. Therefore, the distribution of particles

on both sides of the 0 point will never be symmetrical. From Fig. 2, we can get a piece of information. When the characteristic index is constant, the sufficient external excitation energy the particles can obtain, the more they can move across the barrier to another potential well. That is to say, the greater the noise intensity, the more the particles are in between the potential wells. The higher the crossover frequency, so when we select the parameters of the Lévy noise model, we need to pay special attention to the selection of the feature index α and the noise intensity D.

In this regard, this paper quotes the method of literature [21] to estimate the characteristic index α and the noise intensity D of the Lévy noise model:

$$\mathrm{E}(|\mathrm{X}|^{\rho}) = \frac{\rho \lg \alpha}{\alpha lgD} \mathrm{C}(\rho, \alpha) \tag{8}$$

Where $\mathrm{E}(|\mathrm{X}|^{\rho})$ is the fractional low-order moment, and ρ is the order, $C(\rho,\alpha) = \frac{2^{\rho+1}\Gamma((\rho+1)/2)\Gamma(-\rho/\alpha)}{\alpha\sqrt{\pi}\Gamma(-\rho/2)}$, $-1 < \rho < \alpha \leq 2$.

Let $\mathrm{Y} = \lg|\mathrm{X}|$ $\mathrm{E}(\mathrm{Y}) < +\infty$, the moment generating function is:

$$\mathrm{E}(|\mathrm{X}|^{\rho}) = \lim_{\rho \to 0} \frac{d^{\mathrm{q}}}{d\rho^{q}} \mathrm{E}(|\mathrm{X}|^{\rho}), q \in N^{*} \tag{9}$$

Since Y is only related to α except for the first moment, the first two finite logarithmic moments are listed as:

$$\begin{cases} G_1 = E(|\mathrm{X}|^{\rho}) = \Phi_0\left(1 - \frac{1}{\alpha}\right) + lg\left|\frac{lg\alpha}{\lg Dcosk}\right|^{\frac{1}{\alpha}} \\ G_2 = E\left[(lg|X| - E(Y))^2\right] = \Phi_1\left(\frac{1}{2} + \frac{1}{\alpha^2}\right) - \left(\frac{k}{\alpha}\right)^2 \\ \Phi_0 = \frac{dlg\Gamma(t)}{dt} \\ \Phi_1 = \frac{d^2 lg\Gamma(t)}{dt^2} \end{cases} \tag{10}$$

Let t = 1, then $\Phi_0 = -0.5772$ and $\Phi_1 = 1.6449$ are obtained. The estimated value can be obtained from the above formula:

$$\begin{cases} \widehat{\alpha} = \left(\frac{G_2}{\Phi_1} - \frac{1}{2}\right)^{-\frac{1}{2}} \\ \widehat{D} = e^{(\Phi_0 - G_1)\widehat{\alpha} - 1} \frac{lg\widehat{\alpha}}{cos\widehat{\mathrm{k}}} \\ \left|\widehat{\mathrm{k}}\right| = \left[\left(\frac{\widehat{\alpha}^2}{2} - 1\right)\Phi_1 - G_1\widehat{\alpha}^2\right]^{\frac{1}{2}} \end{cases} \tag{11}$$

To test the effectiveness of the estimation method, the Chambers-Mallows-Stuck (CMS) method is used to generate the Levy noise with $\alpha = 1.5, \mathrm{D} = 1$, and the parameters of α, D are estimated. The estimated results are shown in the figure below (Fig. 3):

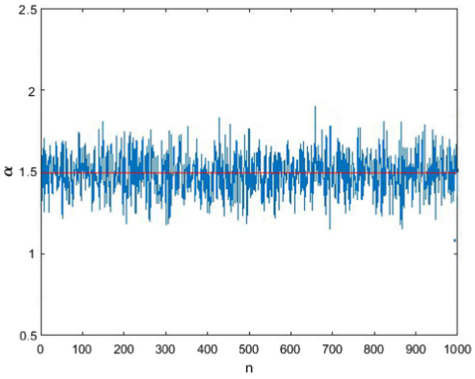

Fig. 3. Estimation of characteristic index α

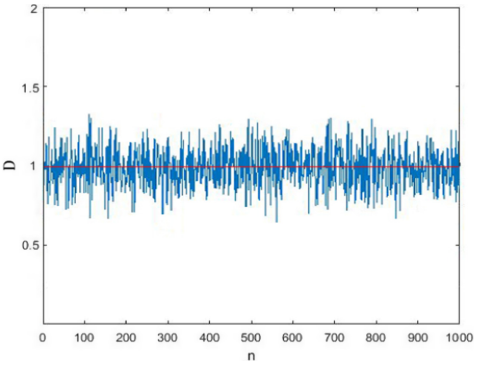

Fig. 4. Estimation of noise intensity D

Where n represents the number of estimates, Fig. 4 and Fig. 5 show that values of α and D are obtained respectively as 1.5026 and 1.1664, which prove that the method can estimate the parameters of interference noise in the actual underwater information sensing environment.

3.2 Improved Signal Sensing Method of Dual Coupling Duffing Oscillator

Although the signal sensing method of the dual-coupled Duffing oscillator improves the speed and accuracy of specific signal-to-noise ratios and threshold solutions, it still has the problem of not being able to estimate the unknown frequency signal parameters, and the signal-to-noise ratio threshold is too high. This paper proposes an improved dual-coupled Duffing oscillator signal sensing method by combining the theoretical knowledge of intermittent chaos and the variable step-size method. The estimated result of the sensed unknown signal frequency is more accurate.

According to the idea of intermittent chaos theory, there is a slight frequency difference between the sensed signal and the built-in driving force of the system, which

can make the sensing system produce a chaotic state and periodic state regular changes. Furthermore, the chaotic oscillator has a solid sensitivity to interference and robust noise immunity. So, this paper proposes to sense the signal through the phase change of the chaotic oscillator. The expression of the signal sensing method of the improved dual-coupled Duffing oscillator is as follows:

$$\begin{cases} \ddot{x_1}(t) + k\dot{x_1}(t) - x_1(t) + {x_1}^3(t) + d(y_1(t) - x_1(t)) = Fcos(\omega t) \\ \ddot{y_1}(t) + k\dot{y_1}(t) - y_1(t) + {y_1}^3(t) + d(x_1(t) - y_1(t)) = \mathrm{Fcos}(\omega t) + Y(t) \\ \ddot{x_2}(t) + k\dot{x_2}(t) - x_2(t) + {x_2}^3(t) + d(y_2(t) - x_2(t)) = \xi \cdot F\mathrm{cos}(\omega t) \\ \ddot{y_2}(t) + k\dot{y_2}(t) - y_2(t) + {y_2}^3(t) + d(x_2(t) - y_2(t)) = \xi \cdot \mathrm{Fcos}(\omega t) + Y(t) \end{cases} \tag{12}$$

Where ξ is the influencing parameter of the chaotic oscillator. $Y(t) = Acos(\omega_1 t)$. The other parameters of the two pairs of Duffing oscillators are the same. We generate the differential timing diagrams $x_1(t) - x_2(t)$ of the two pairs of Duffing oscillators to observe whether the signal has been sensed. The timing diagram should be regular. The change of ξ will not affect the waveform but only the magnitude of the phase difference. When $\xi = 1$, the phase difference disappears, and the two pairs of oscillators are the same. The method will degenerate to for ordinary dual-coupled Duffing vibrators. This article has passed many experiments and finally chose $\xi = 1.001$ to obtain a more intuitive effect.

If $f(t)$ is added as the signal to be sensed to the single Duffing vibrator sensing system, the state equation is:

$$\begin{cases} \dot{x} = \omega y \\ \dot{y} = \omega[-0.5y + x - x^3 + \gamma\mathrm{cos}(\omega t) + f(t)] \end{cases} \tag{13}$$

Where $f(t) = Acos(\dot{\omega} t + \varphi)$, φ is the initial phase of the signal to be sensed, γ is the critical chaos threshold, $\dot{\omega} = \omega + \Delta\omega$, $\Delta\omega$ is the frequency difference between the built-in driving force of the system and the signal to be sensed. The system power is:

$$\mathrm{L(t)} = \gamma\mathrm{cos}(\omega t) + Acos(\dot{\omega} t + \varphi) = \mathrm{P(t)cos}(\omega t + \phi(t)) \tag{14}$$

In the formula (14), P(t) represents the polarization force amplitude:

$$\mathrm{P(t)} = \sqrt{\gamma^2 + 2\gamma Acos(\Delta\omega t + \phi) + A^2}, A \ll \gamma \tag{15}$$

When P(t) changes periodically, if $\mathrm{P(t)} \geq \gamma$, the system is in a large-scale periodic state, and when $\mathrm{P(t)} < \gamma$, the system is in a chaotic state.

In this paper, the Runge-Kutta method is used to analyze the Duffing vibrator sensing system numerically. Through calculation, it is obtained that when the intermittent chaotic frequency difference range of the single Duffing vibrator sensing system is $\left|\Delta\omega/\omega\right| \leq 0.03$, the system is in a state of intermittent chaos. The dual-coupled Duffing oscillator system is $\left|\Delta\omega/\omega\right| < 0.08$ and the improved dual-coupled Duffing oscillator's intermittent chaotic frequency difference range is $\left|\Delta\omega/\omega\right| < 0.09$. Compared

the intermittent chaotic frequency difference range of the three methods, we can see that the method proposed in this paper detect the step size accurately, which makes it meaningful to use the variable step-size method to improve the sensing system further, and it is easier to realize the unknown frequencies. The intermittent chaotic timing diagram of the dual-coupled Duffing oscillator and the method proposed in this paper is shown in Fig. 5:

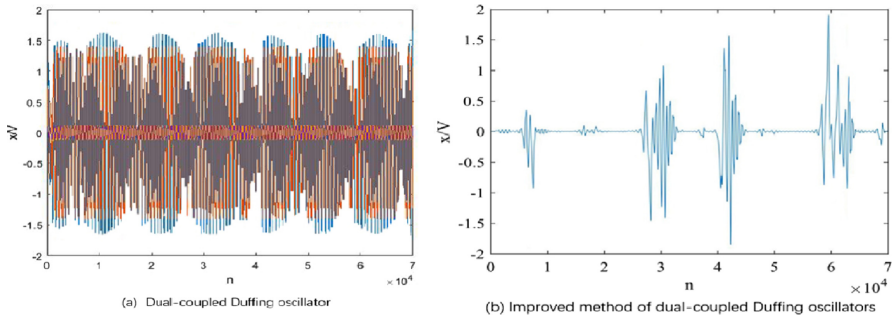

Fig. 5. The intermittent chaotic timing diagram of two methods

Next, we add a variable step-size method based on the above improvements, change the solution step-size, convert the signal into the corresponding discrete sequence of the built-in driving force of the sensing system, and observe the output $x_1(t) - x_2(t)$ Differential timing diagram to determine whether the signal is successfully sensed. The built-in driving force sequence interval of the sensing system is the solution step length of the system, and the sequence interval of the signal to be sensed is T_s ($T_s = \frac{1}{f_s}, f_s$ is the sampling rate of the signal). The sensing result is only related to the sampling rate, so the solution step-size of the sensing system can be changed, it can be directly adjusted to the intermittent chaotic state to complete signal sensing. When the variable step intermittent chaos sensing method is applied, the total strategy terms of Eq. (12) are $\mathrm{Fcos}(\omega t) + A\cos(\omega_1 t)$ and $\xi \cdot \mathrm{Fcos}(\omega t) + A\cos(\omega_1 t)$, and the system is in In the intermittent chaotic state, the solution step-size is $\mathrm{h} = \frac{\dot{\omega}}{lwf_s}, \dot{\omega} = \omega + \Delta\omega, l \in (0.94, 1.06)$. The two strategy items are discretized as:

$$\begin{cases} L_{n_1} = D \cdot \cos\left(\frac{n\dot{\omega}}{lf_s}\right) + A\cos\left(\frac{n\dot{\omega}}{f_s}\right) \\ L_{n_2} = \xi \cdot D\cos\left(\frac{n\dot{\omega}}{lf_s}\right) + A\cos\left(\frac{n\dot{\omega}}{f_s}\right) \end{cases} \tag{16}$$

If $\mathrm{n} \in N^*$, the frequency difference between the built-in driving force and the signal meets the standard of intermittent chaos, the sensing system will appear in the intermittent chaotic state. The specific steps are shown in the figure below:

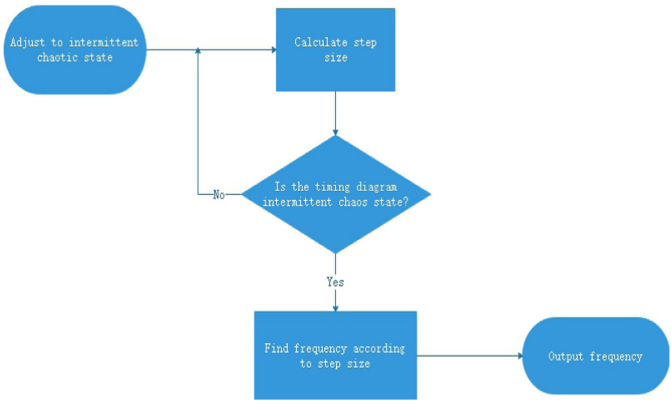

Fig. 6. The specific steps of the sensing system

4 Experiment and Analysis

4.1 Experiment Deployment

To more effectively describe the natural environment interference encountered by underwater information sensing in the real ocean environment, according to the actual underwater data of a reservoir in Hubei, China, measured in the literature [20], through simulation experiments, it is found that when the parameter $\alpha = 1.5, \mathrm{D} = 1$, it is closer to the actual situation. The selection of parameters in this paper is determined accordingly.

This paper uses the Chambers-Mallows-Stuck (CMS) method to generate a Lévy noise model with $\alpha = 1.5, \mathrm{D} = 1$, and build an intermittent chaotic signal sensing system based on an improved variable-step double-coupling Duffing oscillator under Lévy noise interference. Simulation proves the effectiveness and superiority of the sensing system.

After generating the Lévy noise model with $\alpha = 1.5, \mathrm{D} = 1$, take $a_n = 2\pi \frac{1.06^n}{1.06\omega f_s}$ as the solution step-size of the sensing system, and take $Acos(\omega_1 t) + \eta(t)$ as input signal, $\eta(t)$ is the generated Levy noise. According to Fig. 6, the specific steps of the intermittent chaotic signal sensing system of the improved variable-step double-coupled Duffing oscillator established in this paper are as follows:

Adjust parameters. The intermittent chaotic signal sensing system of the variable-step double-coupled Duffing oscillator sets $\mathrm{F} = 0.789, \omega_1 = 1 rad/s, \alpha = 1.001$, $d = 0.2$.

Take $Acos(\omega_1 t) + \eta(t)$ as the input signal into the sensing system, the frequency is set to 1 kHz, and the initial solution step is set to $a_n = 2\pi \frac{1.06^n}{1.06\omega f_s}$, where $\mathrm{n} \in N^*$.

Adjust the solution step size. If the sensing system has an intermittent chaotic state between two adjacent steps a_n and a_{n+1}, then indicates that the signal has been sensed, otherwise go back to the previous step.

If the signal has been sensed, the angular frequencies ω_n and ω_{n+1} corresponding to adjacent steps a_n and a_{n+1} can be calculated by $\omega_n = 1.06^n rad/s$, then the angular frequency of the sensed signal $\ddot{\omega} = \frac{\omega_n + \omega_{n+1}}{2}$ rad/s.

4.2 Performance

We use the dual-coupled Duffing oscillator sensing system and the improved variable-step double-coupled Duffing oscillator's intermittent chaotic signal sensing system established in this paper for signal sensing. The output timing diagram of the two detection methods is shown in Fig. 7 and Fig. 8.

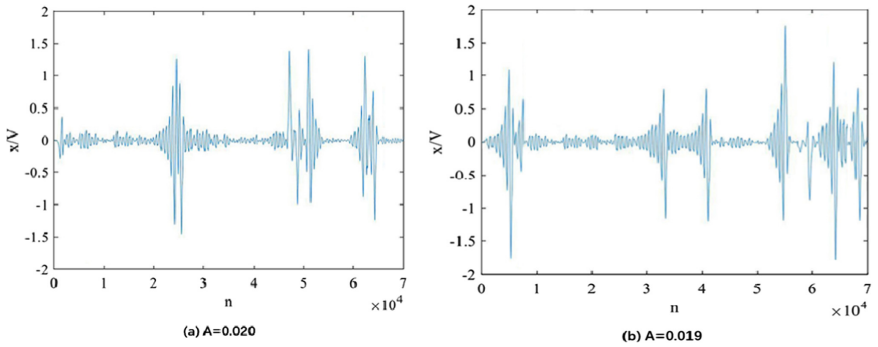

Fig. 7. The output timing diagram of the dual-coupled Duffing oscillator sensing system

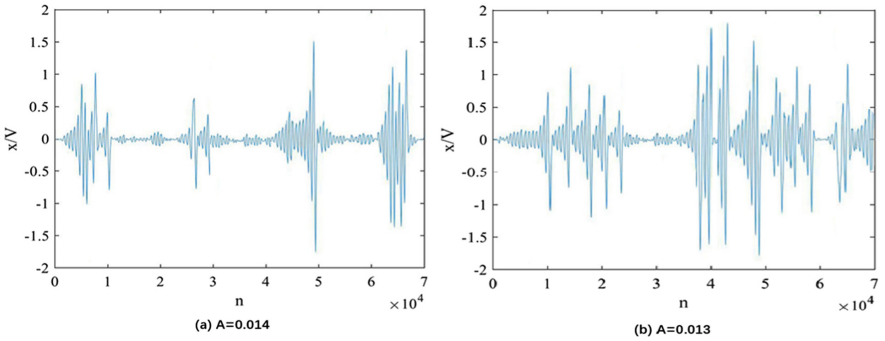

Fig. 8. The output timing diagram of the improved dual-coupled Duffing oscillator sensing system

Figure 7 shows that the dual-coupled Duffing oscillator sensing system appears intermittently chaotic when the adjacent amplitudes A = 0.019 and A = 0.020, indicating that this method can snese periodic signal amplitudes A > 0.020. Figure 8 shows the improved variable step-size double-coupled Duffing oscillator's intermittent chaotic signal sensing system established in this paper when the adjacent amplitudes

A = 0.013 and A = 0.014 appear intermittent chaotic state, indicating that the method can sense periodic signals Amplitude A > 0.014. It shows that the sensing system established in this paper has a broader and more accurate sensing range than the sensing system established in the original method, and comparing Figs. 7 and 8, it can be seen that the output timing diagram of the sensing system established in this paper is clearer and more convenient to observe. The following formula can calculate the minimum signal-to-noise ratio of the two sensing systems:

$$\mathrm{SNR} = 10\frac{A^2}{2\sigma^2} \tag{17}$$

After calculating separately, the SNR of the dual-coupled Duffing vibrator sensing system is –36.98970004 dB. The SNR of the sensing system established in this paper is –40.08773924 dB. It can be seen that the sensing system established in this paper reduces the signal-to-noise ratio threshold of 3.0980392 dB.

The sensing method proposed in this paper can change the standard ratio, form a new solution step size and sensing bandwidth, reduce the number of solution steps, and reduce the amount of calculation. The data of each sensing system is shown in Table 1:

Table 1. Data of each detection system

Method	Common ratio	Number of solving steps	Detection bandwidth
Single Duffing oscillator	1.01	282	$(1.00, 1.01)\omega$
	1.02	197	$(0.99, 1.02)\omega$
	1.03	98	$(0.98, 1.03)\omega$
Double Duffing oscillator	1.05	68	$(0.97, 1.05)\omega$
	1.06	60	$(0.96, 1.06)\omega$
	1.07	57	$(0.95, 1.07)\omega$
Ours	1.06	60	$(0.96, 1.06)\omega$
	1.07	57	$(0.95, 1.07)\omega$
	1.08	35	$(0.94, 1.08)\omega$

It can be seen from Table 1 that the number of solving steps and the amount of calculation of the sensing system established in this paper are obviously the smallest.

Below we verify that the sensing system established in this article can better estimate the frequency of the unknown signal. In the actual underwater signal sensing, multiple signals will be sensed under the same natural environment interference. In this case, when we change the input signal to $0.01cos(10t) + 0.01\cos(20t) + \eta(t)$, the power spectral density is shown in Fig. 9, and the sensing result is shown in Fig. 10.

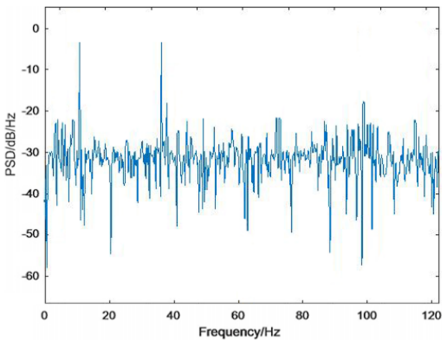

Fig. 9. The power spectral density

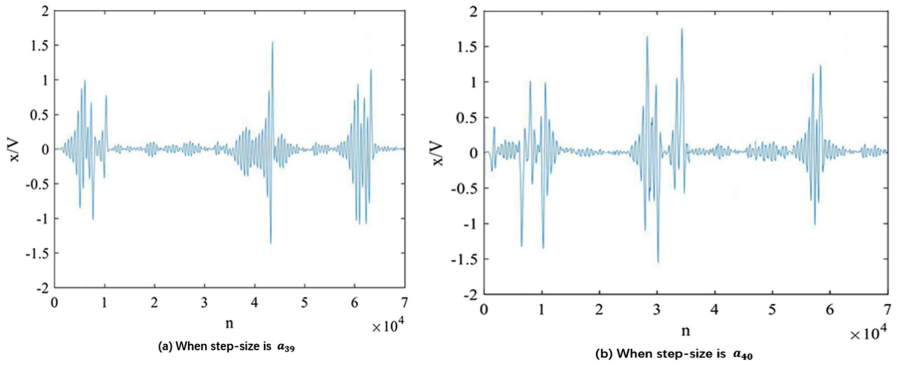

Fig. 10. The sensing results

Figure 10 shows the intermittent chaotic state of the sensing system established in this paper when the adjacent solution steps a = 39 and a = 40. It can be judged that the system senses the signal when the solution steps are 39 and 40, Then can estimate unknown signal frequency. When the signal frequency to be measured is 10 Hz, the adjacent steps are a_{39} and a_{40}, the corresponding sizes of f_{39} and f_{40} are 9.7 Hz and 10.2 Hz. The system's judgment frequency is f_{10} = 9.99 Hz. The calculation error rate is 0.1%; that is, the system can obtain the frequency of the signal to be sensed more accurately under the interference of a healthy natural environment.

5 Conclusion

Aiming at the task of underwater information sensing under solid interference, in this paper, a more general Lévy noise model has been used to better describe the impact characteristics of underwater environmental noise interference in order to describe the natural environment interference of underwater information sensing. Then, an improved dual-coupled Duffing oscillator signal sensing method has been proposed to

detect weak underwater signals with unknown frequencies. This method has lower computational overhead, lower signal-to-noise ratio threshold, and can better estimate the unknown signal frequency. Finally, under the Lévy noise interference, an intermittent chaotic signal sensing system based on an improved variable-step double-coupled Duffing oscillator has been established. A large number of simulation experiments have proved the effectiveness and superiority of the system. The results show that, the lowest signal-to-noise ratio threshold can reach –40.0877, and the frequency estimation error rate is 0.1%.

Acknowledgement. This work was supported in part by the National Natural Science Foundation of China (No. 62072074, No. 62076054, No. 62027827, No. 61902054), the Frontier Science and Technology Innovation Projects of National Key R&D Program (No.2019QY1405), the Sichuan Science and Technology Innovation Platform and Talent Plan (No. 2020JDJQ0020), the Sichuan Science and Technology Support Plan (No. 2020YFSY0010), and the Natural Science Foundation of Guangdong Province (No. 2018A030313354).

References

1. Chen, D., et al.: MAGLeak: a learning-based side-channel attack for password recognition with multiple sensors in IIoT environment. In: IEEE Transactions on Industrial Informatics, to Appear (2021)
2. Zhang, N., et al.: Software defined networking enabled wireless network virtualization: challenges and solutions. IEEE Netw. **31**(5), 42–49 (2017)
3. Zhang, N., et al.: Synergy of big data and 5 g wireless networks: opportunities, approaches, and challenges. IEEE Wireless Commun. **25**(1), 12–18 (2018)
4. Ale, L., et al.: Online proactive caching in mobile edge computing using bidirectional deep recurrent neural network. IEEE Internet Things J. **6**(3), 5520–5530 (2019)
5. Ding, Y., et al.: DeepEDN: a deep learning-based image encryption and decryption network for internet of medical things. IEEE Internet Things J. **8**(3), 1504–1518 (2021)
6. Tian, T.: Sonar Technology. Harbin Engineering University Press, Harbin (2010)
7. Liu, X., Qin, Y.: Modem marine power vs state marine strategy. J. Soc. Sci. 73–79 (2004)
8. Cui, F.: Modern sonar technology. Fundam. Defense Technol. 30–33 (2005)
9. Liu, B., Lei, J.: Principles of Hydroacoustic. Harbin Shipbuilding Institute Press, Harbin (1993)
10. Andrew, R.K., Howe, B.M., Mercer, J.A., Dzieciuch, M.A.: Ocean ambient sound: comparing the 1960s with the 1990s for a receiver off the California coast. Acoust. Res. Lett. Online **3**(2), 65–70 (2002)
11. Korakas, A., Hovem, J.M.: Comparison of modeling approaches to low-frequency noise propagation in the ocean. In: IEEE Proceedings of Oceans 2013. Norway (2013)
12. Shi, J., Zhang, X., Hou, T.: Development trend of low-frequency marine environmental noise level caused by ship noise. Torpedo Technol. 112–116 (2010)
13. Siderius, M., Gebbie, J.: Environmental information content of ocean ambient noise. J. Acoust. Soc. Am. **146**(3), 1824–1833 (2019)
14. Li, N., Li, X.K., Liu, C.H.: Detection method of a short-time Duffing oscillator array with variable amplitude coefficients. J. Harbin Eng. **37**, 1645–1652 (2016)
15. Zhou, S., Lin, C.S.: Application of chaos theory for weak signal of ship detecting. J. Wuhan Univ. **33**, 161–164 (2009)

16. Li, S.Q., Wu, X.Z.: Application of ALE based on FTF algorithm in ship-radiated noise detection. Commun Technol. **50**(6), 1175–1180 (2017)
17. Sun, Q.W., Zhang, J.F.: Weak signal detection based on improved chaotic oscillator system with dual coupling. Comput. Mod. **3**, 17–21 (2012)
18. Shi, Z., Yang, S., Zhao, Z.: Research on weak signal detection based on Van der Pol-Duffing oscillator and cross correlation. J. Shijiazhuang Tiedao Univ. **32**, 66–71 (2019)
19. Xu, W., Hao, M., Gu, X.: Stochastic resonance induced by Lévy noise in a tumor growth model with periodic treatment. Mod. Phys. Lett. **28**(11), 1450085 (2014)
20. Ma, S.: Research on Very Low Frequency Seismic Wave Detection Technology Based on Stochastic Resonance under Levi Noise. Northwestern Polytechnical University, Xian (2018)
21. Ma, X., Nikias, C.: Parameter estimation and blind channel identification in impulsive signal environments. IEEE Trans. Signal Process. **43**(12), 2884–2897 (1995)